

DesignCon 2017

Cost-effective PCB Material Characterization for High- volume Production Monitoring

Yongjin Choi - Hewlett-Packard Enterprise
yongjin.choi@hpe.com

Christopher Cheng - Hewlett-Packard Enterprise
chris.cheng@hpe.com

Yasin Damgaci - Hewlett-Packard Enterprise
yasin.damgaci@hpe.com

Nagaraj Godishala – Hewlett-Packard Enterprise
nagaraj.godishala@hpe.com

Yuriy Shlepnev – Simberian
shlepnev@simberian.com

Abstract

As I/O data rate is pushed beyond 20 Gbps, the process variation of the PCB material property directly affects SERDES margin, thus impacting the overall system quality. The established extraction methodologies of the material property mostly focus on the pass/fail decision, not for monitoring and improving the process control. The goal of the suggested methodology in this paper are twofold: (1) monitoring the material variations with the minimal measurement cost/time and (2) guiding vendors to adjust the manufacturing process based on the monitored statistics. To meet the goal, the new Gamma-T approach utilizes the time or frequency-domain measurements of two transmission line segments and T-resonator with minimal number of cross-sectioning. Two versions of Gamma-T technique are described in this paper: the cost-effective one for the production floor and the precise one for material identification/validation in a lab environment. Both versions are suitable for the material model identification for EDA tools.

Author(s) Biography

YongJin Choi is a Master Technologist at the Storage Division of Hewlett-Packard Enterprise, where he leads the system signal integrity, modeling, material characterization, and SERDES analysis. He received the Ph.D. degree in electrical engineering from North Carolina State University in 2010. His technical interest includes SERDES modeling based on system identification algorithms.

Christopher Cheng received the B.S. and M.S. degrees in Electrical Engineering from Cornell University, Ithaca, NY, in 1987 and 1989 respectively. From 1989 to 1996, Mr Cheng worked for the Sun Microsystems Corporation, CA, USA, as a Signal Integrity engineer. From 1996 to 1999, he worked for Intel Corporation, CA, USA, as a Principal Engineer. In July 1999, he joined 3PAR Data Corporation as a Principal Engineer, Fremont, CA. Currently, he is with Storage Division in Hewlett-Packard Enterprise Company as a Distinguished Technologist.

Yasin Damgaci is a Senior Signal Integrity Engineer at Hewlett-Packard Enterprise and holds a PhD degree in Electrical Engineering from Utah State University. He has been working on methodologies for high-speed interface modelling, system level signal/power integrity design, bring up, validation and debug.

Nagaraj Godishala is currently the Lead System Signal Integrity Engineer with the Storage Division of Hewlett-Packard Enterprise. His work focuses on design, analysis, characterization, optimization, electrical validation and debug of high-speed interfaces. He received his M.S. degree in Electrical Engineering from New Mexico State University and a B.Tech. degree in Electronics & Instrumentation from Kakatiya Institute of Technology & Science, India.

Yuriy Shlepnev is President and Founder of Simberian Inc., where he develops Simbeor electromagnetic signal integrity software. He received M.S. degree in radio engineering

from Novosibirsk State Technical University in 1983, and the Ph.D. degree in computational electromagnetics from Siberian State University of Telecommunications and Informatics in 1990. He was principal developer of electromagnetic simulator for Eagleware Corporation and leading developer of electromagnetic software for simulation of signal and power distribution networks at Mentor Graphics. The results of his research are published in multiple papers and conference proceedings.

1. Material characterization process objectives

The main objective of this work is to develop space efficient method that is accurate up to medium high frequency with high testing throughput while being cost effective using almost all existing testing infra-structures in a high volume PCB manufacturing environment. Only space efficient structure on PCB such as t-line segments can be used. Specifically, the test structures should be composed from the same lines used to connect components. This is because only effective properties can be practically identified due to the anisotropy and inhomogeneity of PCB dielectrics. Time domain method with the existing factory testing infrastructure (TDR/TDT equipment with hand-held probes) should be used. The technique should be high throughput using the handheld probe and TDR scope, no time consuming SMA mounting or VNA calibration. The identification method should also tolerate geometric variations and require limited cross-sectioning. To find out the reasons of possible board failure due to excessive losses, the technique should allow the separation of dielectric and conductor roughness effects. It should complement SET2DIL to help identify material properties once the loss exceeds target specs. The last, but not least, to make it cost-effective, the technique should utilize accurate low-cost EDA tools to design test fixture and do the material model identification. Version with higher accuracy and bandwidth for is needed to complement the cost-effective version for validation purpose in a lab equipped with VNA.

2. Introduction

Design of PCB and packaging interconnects for data links running at bit rates 10-30 Gbps and beyond is challenging. Boards are not manufactured as designed, making accurate measurements from DC to 20-50 GHz is very difficult and accurate modeling over frequency bandwidth from DC to 20-50 GHz is difficult and even not possible in most of the EDA tools. Modeling, manufacturing and measurements are three elements of the design success “fire triangle”. **To have consistency in the modeling and manufacturing, the same material characterization technique must be used at the material model identification and production validation stages.** This is not the case so far. Manufacturers usually use standardized techniques such as SET2DIL [1], Gamma extraction part of SPP technique [1], and Delta-L technique [2] to control the losses only. On the other hand, development teams start using accurate techniques such as GMS-parameters [3] and techniques based on different types of de-embedding (TRL, AFR and ISD) for the material characterization. T-resonator technique originally developed for microwave application was also recently adapted for the digital interconnects [4].

Let's analyze what would be suitable to build unified cost-efficient and accurate technique for the material characterization, suitable for both manufacturers and development labs. SET2DIL [1] technique was originally developed by researches from Intel and typically used by manufactures to control losses at one frequency point. It is basically a cost-effective pass-fail test. It requires the design of nearly perfect, low-reflection launches that may be time-consuming and often not possible in the production environment. Also, it does not have a procedure to figure out the reason of failure (dielectric or copper foil problem). Though, it can be potentially adapted for the broadband material model identification. Short Pulse Propagation [SPP] technique was

introduced in early 90-s by researchers from IBM [5] for characterization of PCB and packaging interconnect losses and dispersion. The standardized technique has nine steps that is too complicated and, until recently, the implementation of the technique was available only in IBM's software that is not available now. Because of that, the model identification part of SPP standard is practically abandoned - only the Gamma extraction part is mostly used, when SPP capability is claimed. We have recently revisited this technique and suggested some simplifications and improvements of the technique to extend the frequency range up to 50 GHz [6]. Unfortunately, Gamma extracted from TDT has defects at lower frequencies and cannot be used to separate dielectric and conductor losses in the same way as with the GMS-parameters or Gamma extracted from S-parameters. Though, some elements of SPP Light [6] are used here to build the new cost-effective technique. Considering the alternatives to SET2DIL and SPP, there is an industry trend to use de-embedding techniques such as TRL (Trough-Reflect-Line) or similar, AFR (Adaptive Fixture Removal), ISD (In Situ De-embedding) for the material characterization. Even a new task group was recently organized by IPC D-24 committee under TM-650 to address the issue of "deficiency" in SET2DIL, SPP and the other material characterization standards. Would de-embedding be a viable alternative for a unified process? A complete de-embedding is very difficult for PCB applications due to large manufacturing variations. Extraction of multiport parameters of test fixture in de-embedding techniques is the most sensitive and error-prone part of any de-embedding technique. But, it would not be needed if only complex propagation constant is required for the material characterization. Also, the complete de-embedding techniques may remove the test fixture effects successfully, but the de-embedded S-parameters of a line segment still have reflections due to the mismatch in the segment S-parameters normalization and the frequency-dependent characteristic impedance of the transmission line. The material characterization results will depend on this reflection. An opposite to the use of complete de-embedding is characterization without de-embedding at all [2]. Attenuation and phases of two line segments in Delta-L technique are simply subtracted and divided by length difference to have per unit length parameters. The technique has strong dependency on the reflections from connectors, probes, launches and transmission lines. Design of transparent launches for any stackup is very challenging and may not be realistic in the production environment that is similar to SET2DIL technique. In addition, it requires S-parameter measurements for two line segments. If S-parameters are already measured, GMS-parameters [3] and SPP Light [6] would be more accurate and much less sensitive to the reflections alternatives.

The bottom line is we did not find readily available technique that satisfies our requirements for the material characterization formulated in the previous section. Thus, a hybrid technique composed from the elements of existing methods is proposed here. New technique uses complex propagation constant (Gamma) extraction from TDT or S-parameters complemented with the T-resonator technique to separate dielectric and conductor losses.

3. Broadband material models

First of all we have to identify material models that can be used for the broadband analysis of PCB/packaging interconnects. One broadband model for dielectrics and one model for conductor roughness are described here as the most commonly used. **Models**

like that have to be the outcome of the model identification process, not just frequency points that are typically provided by the dielectric manufacturers. There is usually no information available from manufacturers that is suitable for electrical modeling of the conductor surface roughness.

Wideband Debye (aka Djordjevic-Sarkar or Swensson-Dermer) and multi-pole Debye models [7] are dielectric models often used for broadband analysis of PCB and packaging interconnects. Expression for complex permittivity of the wideband Debye model can be written as follows [7]:

$$\varepsilon(f) = \varepsilon(\infty) + \frac{\varepsilon_d}{(m2 - m1) \cdot \ln(10)} \cdot \ln \left[\frac{10^{m2} + j \cdot f}{10^{m1} + j \cdot f} \right] \quad (3.1)$$

where f is frequency (the original formula of [7] is adjusted to use linear frequency instead of the radial for convenience). Values of dielectric constant at infinity $\varepsilon(\infty)$ and parameter ε_d can be defined with dielectric constant and loss tangent at one frequency point. Values of $m1$ and $m2$ define position of the first and last pole in the continuous spectrum defined by the model. Those are typically set to very low and very high values outside of the frequency band of interest ($m1=4$, $m2=12$), but they may be also treated as variables in the identification process.

If model (3.1) does not capture observed dielectric dispersion, universal multi-pole Debye model can be used [7]. Multipole models with complex poles (Lorentzian for instance) and Cole-Cole model may be also considered as the alternatives to the wideband and multi-pole Debye models.

To simulate the effect of conductor roughness, modified Hammerstad [8] or Huray's snowball [9] roughness correction coefficients are often used. They can be applied to either conductor surface impedance locally [8] or to the internal conductor impedance part of the global impedance per unit length of multiconductor line (if static field solver is used). Modified Hammerstad correction coefficient can be expressed as follows [8]:

$$K_{rh} = 1 + \left(\frac{2}{\pi} \cdot \arctan \left[1.4 \left(\frac{\Delta}{\delta} \right)^2 \right] \right) \cdot (RF - 1) \quad (3.2)$$

It has two parameters: Δ or surface roughness (SR) parameter (may be associated with rms peak to valley value for regular copper) and roughness factor RF (maximal possible increase of conductor losses due to roughness). Note that classical Hammerstad model has $RF=2$ and just one parameter, but not very useful for characterization of rough PCB copper [8]. An alternative to the model (3.2) is the impedance correction coefficient based on the Huray's snowball model [9] simplified in [8]. Other roughness correction coefficients can be also considered [8], but they all require the identification process. As the alternative to the correction coefficients, effective roughness dielectric (ERD) layer [10] can be used to simulate the roughness effect. Parameters of ERD layer can be computed from micro-photographs of the surface or identified similar to the roughness correction coefficients.

4. T-resonator technique

T-resonator is a well-known approach to extract the dielectric properties of the PCB material at the resonance frequencies [4], [11]. First, we extract the dielectric constant of the material from this resonator. The resonance frequencies of the T-resonator is defined

by the stub length in the structures shown in Fig. 5.1 or Fig. 6.1. Here we are using the stripline structure to reduce the dispersion and radiation loss occurring with the microstrip one. As the structure is a quarter-wave stub resonator, it resonates at the odd multiples, f_n of the quarter-wavelength frequency. The stub length L_q is equal to the quarter wavelength:

$$L_q = \frac{\lambda_q}{4} = \frac{\lambda}{4\sqrt{\epsilon_r}} = \frac{nc}{4f_n\sqrt{\epsilon_r}} \quad (4.1)$$

where ϵ_r is the effective dielectric constant, c is the speed of light, and n is odd integers. For example, with $n=1$, $\epsilon_r=4$, and $f_1=500\text{MHz}$, the stub length, L_q becomes 7.5cm (2.95 inches). Here $\epsilon_r=4$ is the initial guess. If the measured f_1 is deviated from the designed 500MHz, we need to calculate the actual value of ϵ_r . The more accurate stub length and ϵ_r can be calculated considering the T-junction discontinuity and the open-end transmission effect.

The next step is to extract the loss-tangent ($\tan\delta$) of dielectric constant at the main resonant frequency (f_1). In general, total attenuation (α_T) of the transmission line is described as the sum of conductor (α_C) and the dielectric attenuation (α_d), as long as the loss caused by the surface roughness is insignificant. The surface roughness would be very small if the resonant frequency is roughly less than ~1GHz. So,

$$\alpha_T = \alpha_C + \alpha_d \quad (4.2)$$

By using $Q = \pi/\alpha\lambda_q$, the above equation is converted into the quality factor forms:

$$\frac{1}{Q_T} = \frac{1}{Q_C} + \frac{1}{Q_d} \quad (4.3)$$

Since $Q_d = 1/\tan\delta$,

$$\tan\delta = \frac{1}{Q_T} - \frac{1}{Q_C} \quad (4.4)$$

Using the closed-form α_C [12], the conductor quality factor $Q_C = \pi/\alpha_C\lambda_q$ is easily calculated. The total quality factor $Q_T (= f_1/\Delta_{3db})$ around the resonant frequency f_1 is also easily calculated by measuring the 3dB bandwidth (Δ_{3db}) around f_1 .

To get the more accurate results, the loading effect in Q_T needs to be calibrated out, but the difference is minimal. The extracted dielectric parameters are used as the reference data point at the resonance frequency when generating the Wideband Debye model.

5. Identification with Gamma-T technique

We start with the brief description of the hybrid technique and then proceed with the details. First, T-resonator is used to identify the loss tangent (LT) at lower frequency, where the conductor roughness effect can be neglected. Then, the complex propagation constant (Gamma) is extracted and used for the material model identification following the SPP Light technique or GMS-parameters procedure [3], [6] by simple matching of the measured and simulated Gammas. To separate the dielectric and conductor losses, the LT value identified with the T-resonator is used to define dielectric losses in the Wideband Debye model. All additional losses are attributed to the conductor surface roughness model, that is identified by matching real part of Gamma. Two version of the hybrid

technique are described here: the cost-effective one for the production floor equipped with TDR scope and the precise one for the development lab equipped with VNA.

To extract the loss tangent at low frequency, T-resonator shown in Fig. 5.1 is used – resonator length is adjusted to have resonance at a frequency below 1 GHz, where the conductor roughness effect can be neglected. To extract the complex propagation constant or Gamma, two transmission lines with identical launches, cross-sections and different lengths as shown in Fig. 5.1 are used. The structures are similar to the structures used in SPP or GMS-parameters technique [3], [5], [6]. An optimal line length difference ratio should be about 1:3. The short line length limits the lowest frequency if Gamma is extracted from TDT (the low frequency defect is related to the observed t-line resistance and is discussed later). In case if Gamma is extracted with S-parameters, the shortest segment length should be defined to have minimal direct probes and launches interaction.

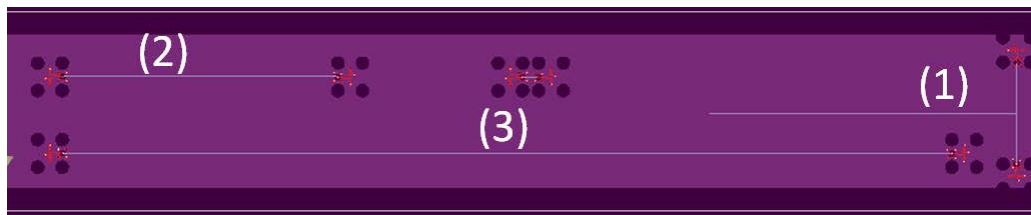


Fig. 5.1. Example of test fixtures for Gamma-T process: T-resonator (1) and two transmission line segments (2) and (3).

For Gamma extraction, the transmission lines can be a single-ended or a differential, strip or microstrip. Trace width should be close to the one used for the routing of actual board. Design of the launches is important but not so critical as in SET2DIL or Delta-L techniques because the Gamma extraction with TDT uses partial de-embedding of the launch reflections and the extraction with S-parameters de-embeds the launches effect completely. Hand-held probes can be used for the cost-effective or production version. For the precise material characterization in lab, RF probes with a probe station or SMA connectors should be used. To extract Gamma, TDR/TDT can be used for the cost-effective version and S-parameter measurements for precise/lab version. **The hybrid Gamma-T procedure is a simple four-step process outlined and illustrated below.**

Step 1 - Prequalification: Measure TDR and TDT step responses of line segments (cost-effective) or measure S-parameters and compute TDR. Select the responses of two segments that meet the target impedance differences: less than 5 Ohm for 20 GHz bandwidth, and less than 3 Ohm for 50 GHz frequency bandwidth. Example of the pre-qualification on a test-board is shown in Fig. 5.2.

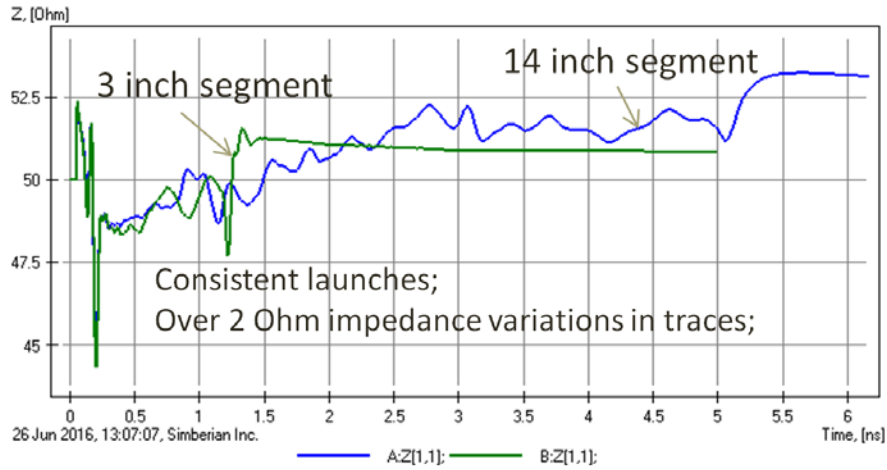


Fig. 5.2. Example of test fixtures pre-qualification with TDR. The launches are reflective, but consistent. About 2 Ohm impedance variation is acceptable for the Gamma extraction.

Step 2 – Gamma extraction for cost-effective version: The measured at step 1 TDT responses of the pre-qualified structures are optionally filtered and converted into short pulse response as illustrated in Fig. 5.3.

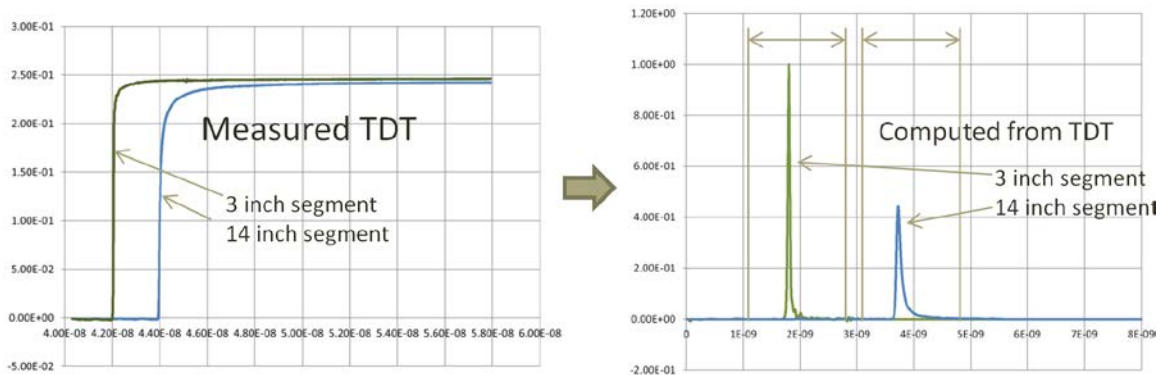


Fig. 5.3. Example of TDT measured for two transmission line on a test board. The TDT responses are filtered from the measurement noises and converted into pulse responses with smoothing 7-point differentiation. Windowing is shown by arrow on the right plot – the same window is used for the short and long segments: $T_{flight} \pm 1.0 * T_{flight_short}$.

To avoid the use of additional equipment for measuring a pulse response or convert TDT response into a pulse response as suggested in SPP standard [1], we suggest filtering out noise from the TDT response and then use multi-point smoothing derivatives. **Gaussian filter can be used to remove the measurement noise.** The Gaussian filter has smooth frequency-domain and time domain responses and can be considered as the infinite pole Bessel-Thompson filter. The responses decay to zero rapidly and have simple analytical formulas in frequency and time domains:

$$v(f) = v_0 \cdot \exp(-2 \cdot \pi^2 \cdot f^2 \cdot \sigma^2) \quad (5.1)$$

$$v(t) = v_0 \cdot \exp\left(-\frac{(t-t_0)^2}{2 \cdot \sigma^2}\right) \quad (5.2)$$

where v_0 is the value at DC in (5.1) or the Gaussian pulse magnitude in (5.2), σ is “standard deviation”, and f is frequency, t is time and t_0 is delay.

The filter parameters can be defined in the frequency domain as follows. We specify cut-off frequency f_{cut} at which the filter response drops by $\alpha = \frac{v(f_{cut})}{v_0}$. Those two

parameters can be used to define the standard deviation in (5.2) as follows:

$$\sigma = \frac{\sqrt{-2 \cdot \ln(\alpha)}}{2 \cdot \pi \cdot f_{cut}} \quad (5.3)$$

To define the filter impulse response for the convolution in time domain, the minimal pulse starting value $v_{min} = v(t-t_0)$ can be used to define the delay t_0 as follows:

$$t_0 = \sigma \cdot \sqrt{-2 \cdot \ln(v_{min})} \quad (5.4)$$

This defines the filter pulse response in time domain (5.2) with $v_0 = 1$. To “filter” the TDT signal, it has to be convolved with the Gaussian pulse (5.2). Recommended values for the Gaussian filter: f_{cut} is equal to the maximal model frequency multiplied by 2, $\alpha = 0.01$ or -40dB, and $v_{min} = 10^{-7}$.

Alternatively or complementary to the Gaussian filtering, smoothing derivatives can be used to convert TDTs into the pulse responses numerically. Pulse response zero adjustment may be also needed in some cases (see SPP standard for details [1]). **Next the double reflections from the launches have to be removed with the windowing and smooth transition to zero of the remaining response.** The windowing illustrated in Fig. 5.3 can be considered as a partial de-embedding. Sensitivity of the Gamma extraction to the reflections at the launches is investigated in the next chapter. **Finally, we convert the processed pulse responses into frequency domain with the Fast Fourier Transform $V(f) = fft(V(t))$ and compute the complex propagation constant as follows:**

$$\Gamma(f) = \alpha(f) + j \cdot \beta(f) = \frac{1}{\Delta L} \ln\left(\left|\frac{V_{long}(f)}{V_{short}(f)}\right|\right) + j \cdot \frac{1}{\Delta L} \arg\left(\frac{V_{long}(f)}{V_{short}(f)}\right) \quad (5.5)$$

Here $\Gamma(f)$ is the complex propagation constant (Gamma), $\alpha(f)$ is attenuation in Np/m, $\beta(f)$ is phase constant in rad/m, ΔL is the line segments lengths difference in m,

$V_{long}(f)$ is the Fourier transform of the pulse response of the long line segment,

$V_{short}(f)$ is the Fourier transform of the pulse response of the long line segment.

Example of the pulse response conversion into Gamma is shown in Fig. 5.4.

This step is the same as the one in the recently suggested by authors SPP Light procedure [6]. Note that the extracted Gamma has some defects at lower frequencies that will be discussed in the sensitivity analysis chapter.

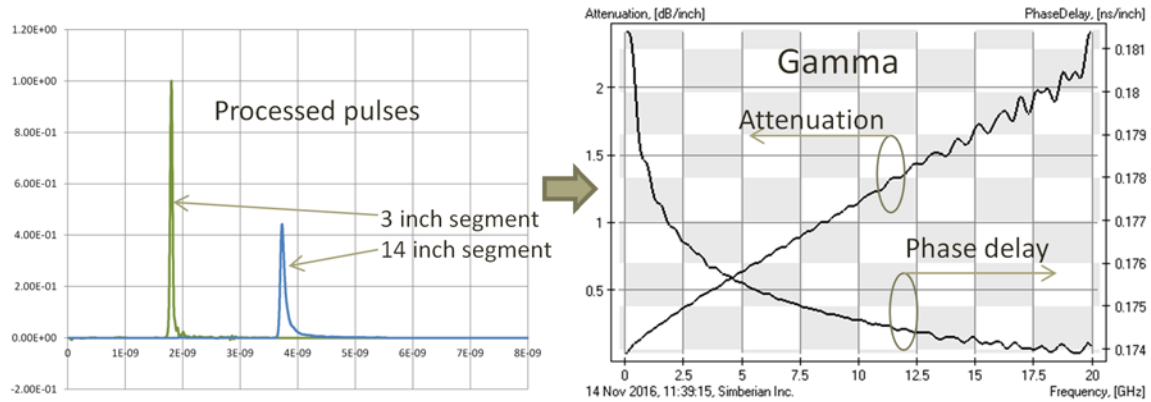


Fig. 5.4. Example of complex propagation constant extraction from two pre-processed pulse responses of 3 and 14 inch transmission line segments. Gamma is converted into attenuation in dB and phase delay to see the details.

Step 2 – Gamma extraction for precise version: Extract Gamma from GMS-parameters computed from S-parameters of two segments as described in [3], [6], [13]. The procedure is illustrated in Fig. 5.5 and Fig. 5.6. Note that GMS-parameters extraction from S-parameters of two line segments is technically a step in any TRL-type de-embedding process. The results are S-parameters of the line segment difference normalized to the un-known characteristic impedance of the transmission line called Generalized Modal S-parameters or GMS-parameters. Taking the logarithm of the GMS-parameters and dividing it by the lengths difference, we can easily compute Gammas for a single-ended as well as for multi-conductor lines with any cross-section.

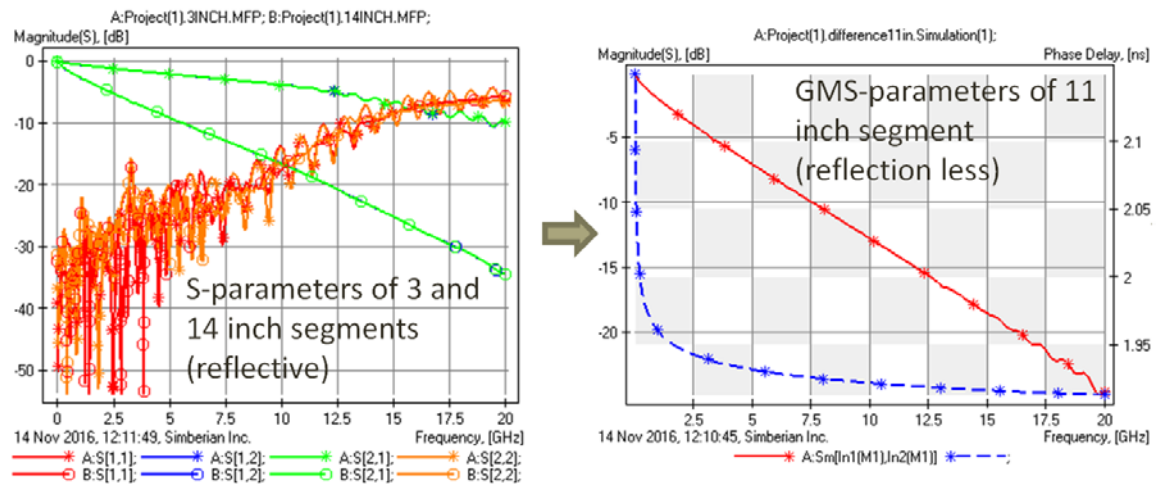


Fig. 5.5 Example of GMS-parameters extraction from S-parameters measured for two line segments. The original structures are reflective (non-zero S11 at the left plot) and GMS-parameters have only transmission and zero reflection (right plot).

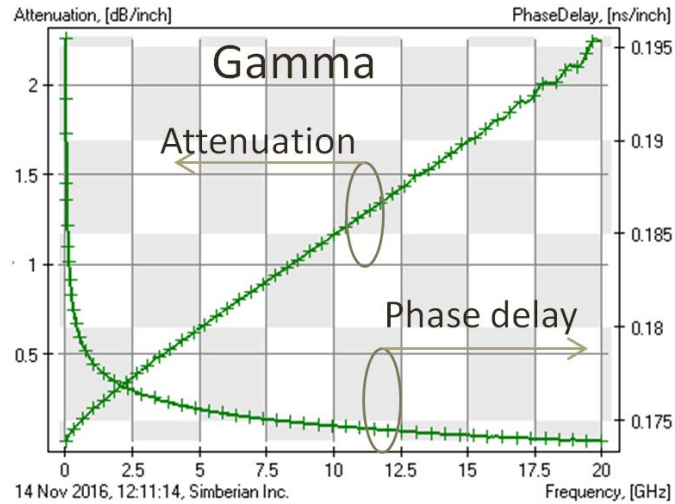


Fig. 5.6. Example of the complex propagation constant extracted from GMS-parameters shown in Fig. 5.5.

Note that the Gamma extraction is also a part of the TRL-type de-embedding process. It can be used for the material parameters extraction as suggested [14]. Though, the procedure is based on approximate formulas suitable for specific MIC application. It is not suitable for PCB/package realm. Here we suggest using a field solver to account for the geometry peculiarities as outlined in step 3 for the precise model identification.

Step 3 (common) - Cross-sectioning: To proceed with the model identification in step 4, we have to know geometrical dimensions of the transmission line. PCB manufacturing variations are notoriously large [15]. Traces are manufactured as not rectangular, but rather trapezoidal or other shapes due to the under or over-etching. To compensate for the etching effect and to adapt the design to a particular batch of dielectric, the manufacturers do the geometry adjustments to get the target impedance for single-ended or differential line. To have accurate material models at the end, all that has to be taken into account in the model of t-line cross-section. The board has to be cross-sectioned and the dimensions measured as shown in Fig. 5.7.

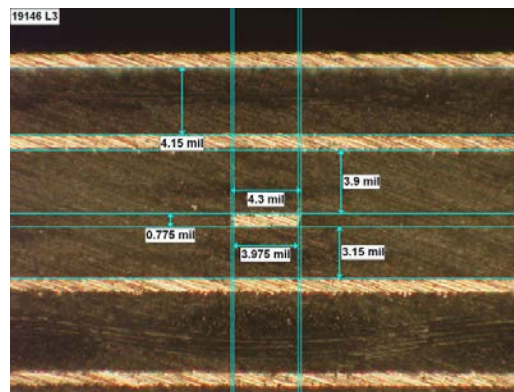


Fig. 5.7. Example of cross-sectioning and dimension measurement for precise material characterization. The trace has “hat” shape in this case.

Taking into account the sensitivity of the proposed technique to the manufacturing variations, the cross-sectioning has to be done once for a new batch of dielectric material, to account for the manufacturer's adjustments. This is when it is typically done by the board manufacturer in any case for the "impedance" correction procedure.

Step 4 (common) - Material model identification: Build cross-section model in a field solver and match the computed Gamma with the measured Gamma by changing dielectric and conductor roughness model parameters. To separate the dielectric and conductor losses, use loss tangent identified with the T-resonator to define the Wideband Debye model. Next adjust Dk to match phase delay and adjust roughness model parameters to match insertions loss. Example of the Gamma matching for the material parameters identification is provided in Fig. 5.8.

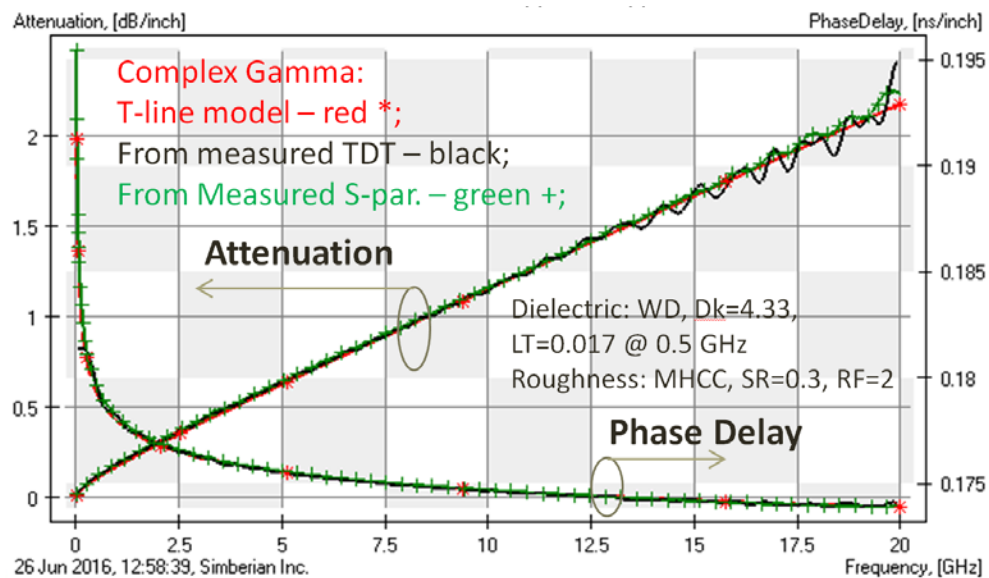


Fig. 5.8. Example of the dielectric and conductor roughness model identification with the cost-effective (from TDT) and with the precise (from S-parameters) techniques. Both techniques produced Wideband Debye model for dielectric with $Dk=4.33$ and $LT=0.017$ @ 0.5 GHz and Modified Hammerstad Correction Coefficient (MHCC) with $SR=0.3$ and $RF=2$ for the conductor roughness.

With the Gamma extracted from GMS-parameters, there is another way to separate the dielectric and conductor losses suggested by S. McMorrow. It goes as follows. First, use loss tangent and Dk from the material spreadsheet and adjust Dk in the Wideband Debye model to match phase or group delay. Next, adjust the loss tangent of Wideband Debye model and possibly bulk resistivity of conductor to match the insertion loss over the frequency bandwidth from 0.01 to about 0.5 GHz. That will give the effective loss tangent. Next, adjust the conductor roughness model by matching the attenuation from 1-5 GHz up to the highest frequency of the measured Gamma. The T-resonator can be used as an additional test fixture to verify the results of extraction with Gamma.

6. Sensitivity to strip width

The boards are not manufactured precisely as designed due to the process adjustments and statistical variations [15]. To get the information about the process and etching adjustments we can use cross-sectioning – once per each batch of materials. It is practically not possible to do it for each manufactured board. Thus, the material identification technique should not be very sensitive to such manufacturing variations. We will investigate the sensitivity of the Gamma-T approach with the numerical experiment. Parameters of the structure with varying strip width will be computed and used to identify the material parameters assuming that we do not know that the strip width is changed.

We start with the T-resonator first, compute S-parameters of the resonators with varying strip width and use them to identify the effective loss tangent. The initial geometry of the T-resonator is shown in Fig. 6.1.



Fig. 6.1. The original geometry of T-resonator.

To evaluate the identified loss tangent variations with the strip width variation, we will adjust the strip with by -20%, -10%, +10% and +20%. The results of numerical analysis are shown in Fig. 6.2. We can see that changes in the strip width affect the resonance magnitude. Though, the resonance is at the same frequency about 593 MHz. The extracted loss tangent is shown in Table 6.1. We observe variation of the loss tangent within 2.6% for 20% variation of strip width and about 2% for 10% variation of the strip width. This is less than 0.05 dB/inch variation in the attenuation.

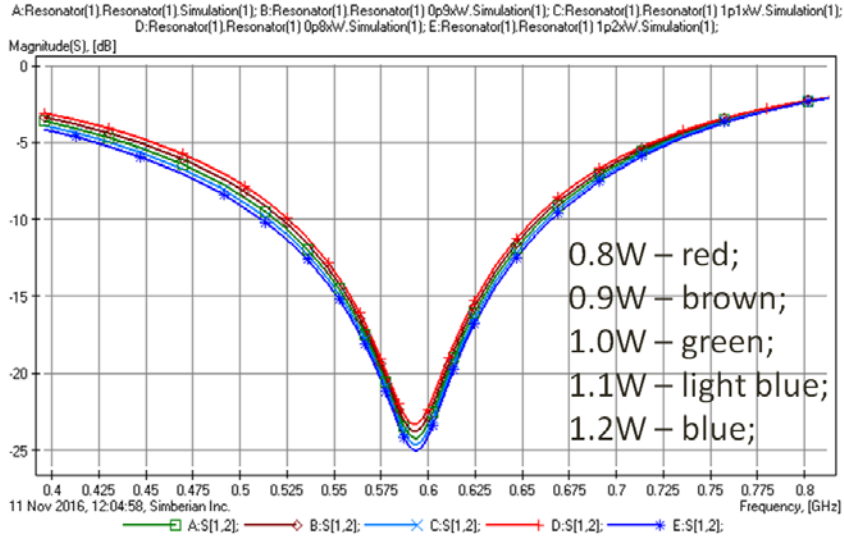


Fig. 6.2. The first transmission resonance dependency on the variation of the strip width.

Table 6.1. Effective loss tangent (LT) at 593 MHz identified with the T-resonator with different strip widths.

| strip width | LT | variation |
|-------------|--------|-----------|
| 0.8W | 0.0196 | 2.60% |
| 0.9W | 0.0195 | 2.10% |
| 1.0W | 0.0191 | 0% |
| 1.1W | 0.0195 | 2.10% |
| 1.2W | 0.0195 | 2.10% |

The variations in the identified LT are acceptable, and actually within the expected material properties variations. This experiment is done for relatively lossy dielectric and should be done for the other types of dielectrics and manufacturing variations if necessary. Also note that the difference in the predicted losses that comes from the strip width variations will be compensated by the conductor roughness model during the insertion loss matching step.

To investigate the sensitivity of the Gamma extraction to possible strip width variation within 20%, we modeled the transmission line cross-section shown in Fig. 6.1 with different strip widths and use the real part of the computed Gamma to identify the effective loss tangent for Wideband Debye model defined at 1 GHz. Strip with the original width W is used to match Gamma of the strip with the adjusted width. The attenuation plots are shown in Fig. 6.3. and the extracted values of the effective loss tangent are provided in Table 6.2. The imaginary part of Gamma and, thus, the phase delay are practically not changing for strips with different width.

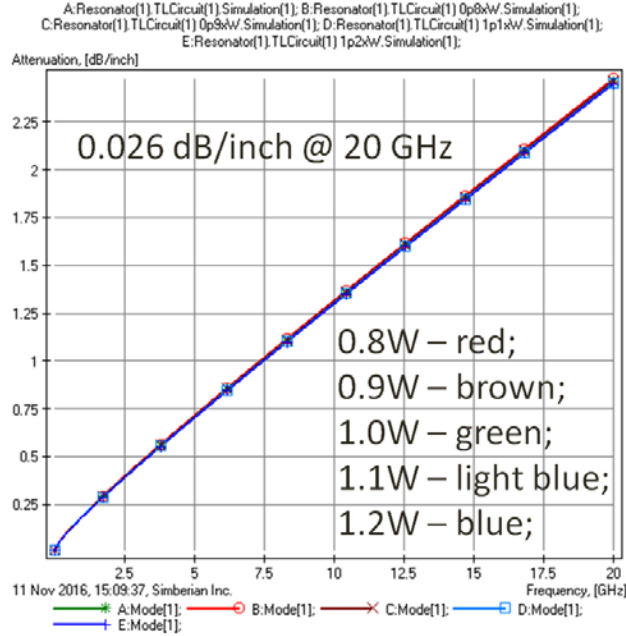


Fig. 6.3. Sensitivity of the attenuation to strip line width. 20% variation in strip width causes only 0.026 dB/inch variation in the attenuation. The dielectric loss dominates in this example.

Table 6.2. Effective loss tangent (LT) at 1 GHz identified with Gamma computed for t-line with different strip widths.

| strip width | LT | variation |
|-------------|---------|-----------|
| 0.8W | 0.02197 | +0.97% |
| 0.9W | 0.02185 | +0.42% |
| 1.0W | 0.02176 | 0% |
| 1.1W | 0.02171 | -0.24% |
| 1.2W | 0.02163 | -0.58% |

With the strip width variation 20%, the identified loss tangent at 1 GHz is within 1% variation, or about 0.026 dB/inch at 20 GHz. This is small value. We used the loss tangent here just for the comparison purpose. Following the process outlined in the previous chapter, the 0.026 dB/inch at 20 GHz will cause practically insignificant differences in the conductor roughness model.

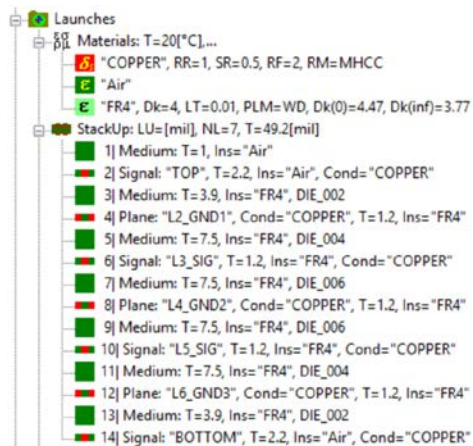
We can conclude that the suggested technique has acceptable sensitivity to possible manufacturing variations of strip width for lossy dielectrics. Sensitivity for the low-loss dielectric has to be investigated further.

7. Sensitivity to launch reflections

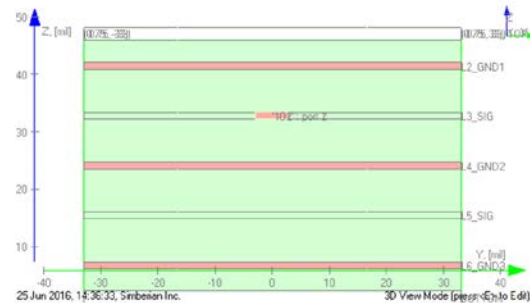
Material characterization technique such as SET2DIL and Delta-L heavily rely on the perfect probe of connector launch design. It can be easily done for a simple test board by the experienced engineer. However, it is difficult to do for stackups with large layer

count. It requires the use of electromagnetic software. With some exceptions [16], such tools are very expensive and have a steep learning curve. Doing a non-reflective launch design in the production environment is not practical. Thus the material characterization technique should tolerate substantial reflections from the launches. To investigate the sensitivity of the Gamma extraction to the launch design, we will use a numerical experiment with the stackup and material properties shown in Fig. 7.1. The transmission line characteristic impedance is close to 50 Ohm.

Let's first extract Gamma from TDTs of 2 inch and 6 inch transmission lines without any launches – this is going to be the best case scenario (unrealistic). We use Gaussian step with 20 ps 10-90% rise time as the stimulus and follow the Gamma extraction procedure. The results are shown in Fig. 7.2. for the extraction without any windowing and with the windowing as described in the Gamma extraction chapter. Without the windowing, we obtain the result that is practically identical to the attenuation and phase delay computed for the transmission line shown in Fig. 7.1. This is expected. However, if we window the time domain response, we get some defects at low as well as at high frequency as illustrated in Fig. 7.3. The phase delay “saturates” at the lower frequencies – this is also expected, because the window is too short for TDT to converge to the t-line resistance at lower frequencies. In addition to the low-frequency defect we also observe some oscillations at the high frequencies.



6 mil strip line, 2 and 6 inch segments



Dielectric: Wideband Debye, Dk=4, LT=0.01 @ 1 GHz;
Conductor roughness: MHCC, SR=0.5, RF=1

Fig. 7.1. Stackup structure and material parameters for the analysis of sensitivity of Gamma extraction to the launch design.

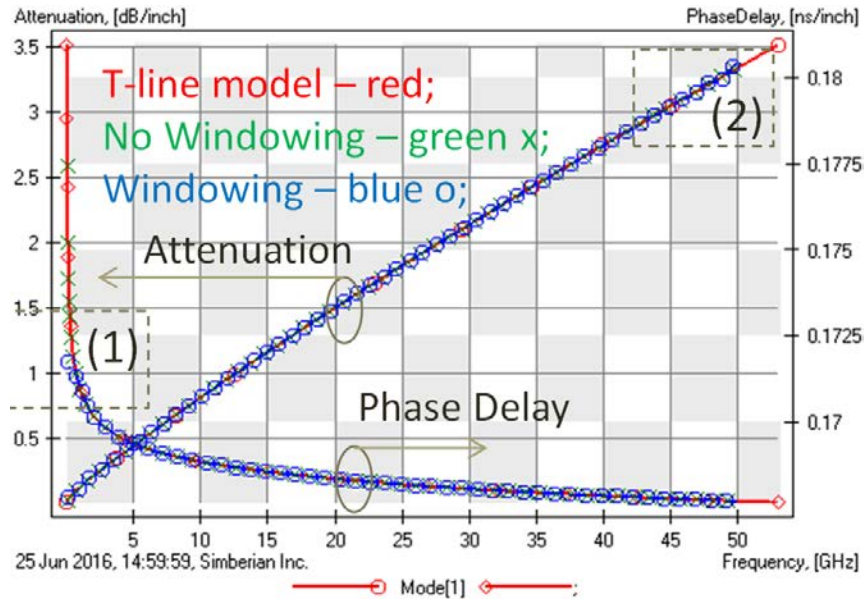


Fig. 7.2. Gamma extracted from TDTs of 2 and 6 inch transmission line segments without windowing and with the windowing. Box (1) highlights low frequency defect and box (2) high frequency defects caused by the windowing.

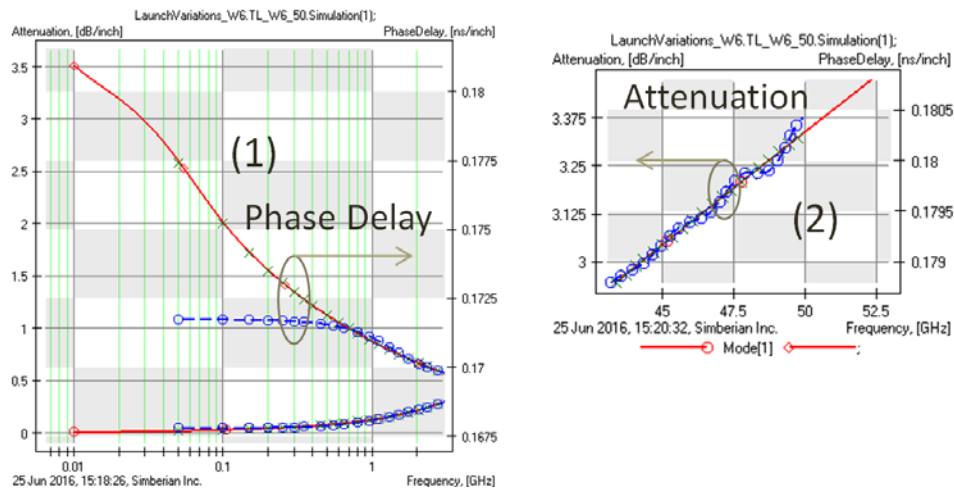


Fig. 7.3. Low (left plot) and high frequency defects caused by windowing during Gamma extraction with the best case scenario (2 and 6 inch lines without launches).

If the windowing causes the defects, why do we need it? Obviously, we would get the excellent results in case of non-reflective launches, but what about more realistic cases. Let's construct 3 launches with different amount of reflection and see what would happen with the extracted Gamma. Insertion loss of 2 inch and 6 inch segments without launches and with 3 different launches are shown in Fig. 7.4. Launch 1 is well designed, launch 2 is not so good (not much design efforts) and Launch 3 is the launch without any design efforts at all and with a stub that is not back-drilled (oops).

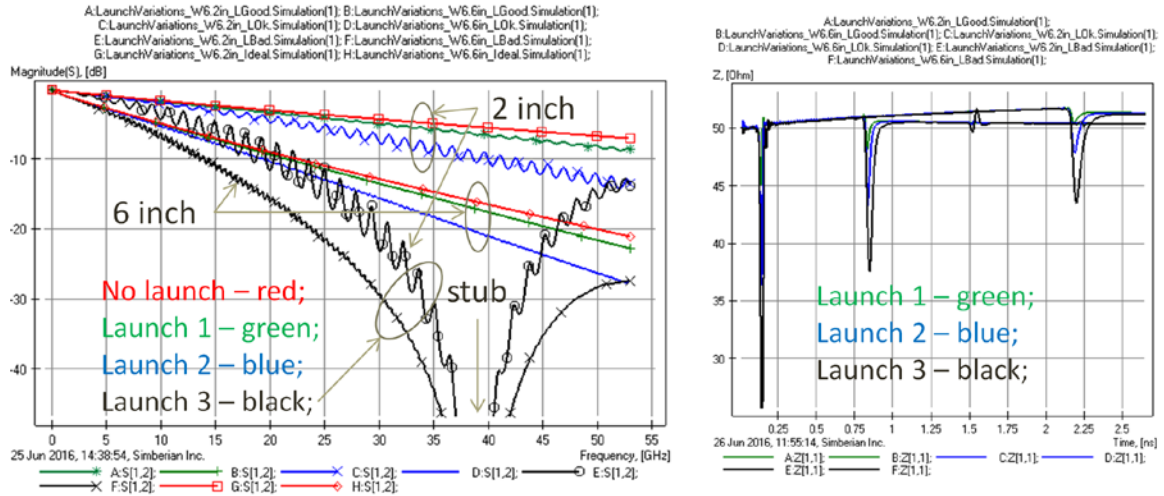


Fig. 7.4. Insertion loss (left plot) and TDR (right plot) for 2 and 6 inch transmission line segments with different launches for Gamma extraction.

Let's try to extract Gamma from TDT without windowing. The result is shown in Fig. 7.5. We can see that the good launch 1 produces the accurate Gamma – attenuation and phase delay extracted from 2 and 6 inch segments (green + in Fig. 7.5) are very close to the parameters of the original transmission line. However, more realistic launch 2 produces oscillations starting from about 10 GHz (blue lines in Fig. 7.5). If we keep the stubs on the launch, the results become practically unusable above 3-5 GHz (black lines in Fig. 7.5).

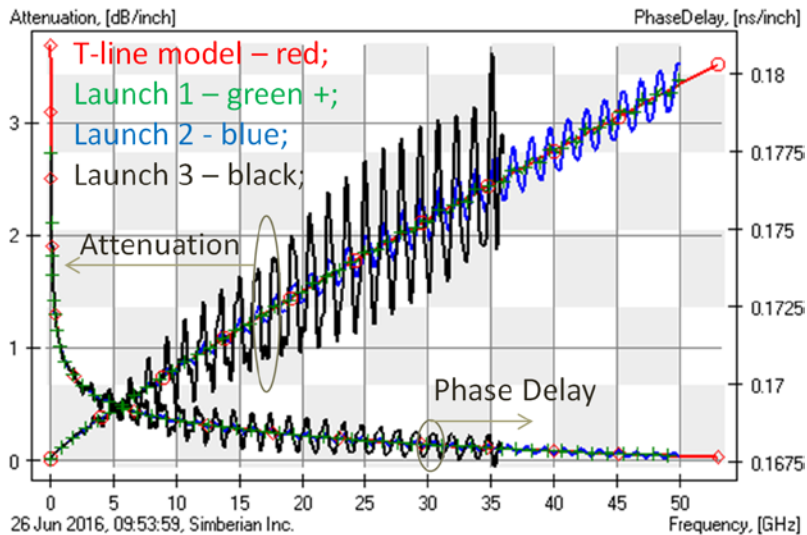


Fig. 7.5. Gamma as attenuation and phase delay extracted from TDTs of 2 and 6 inch segments equipped with different launches and without windowing in time domain.

The reason of this failure is the double reflections observed on the pulse response in Fig. 7.6. The pulse travels from one end of the segment to another and some energy is reflected by the launches, goes back to the source, reflected again and appears as the

delayed oscillation shown in Fig. 7.6 It happens because of the reflective launches and not enough attenuation in the transmission line segments. The double reflection effect can be reduced by using longer lines, but it may take too much space that is not an option on the production boards. The second option is to window the pulse response to get rid of the reflections as illustrated in Fig. 7.6. Gamma computed with the windowing is shown in Fig. 7.7. The results are much better now – even the case with the launch 3 with stubs produced acceptable attenuation and phase delay up to 36 GHz. Though, the windowing causes the same low-frequency defect as in the case without the windowing.

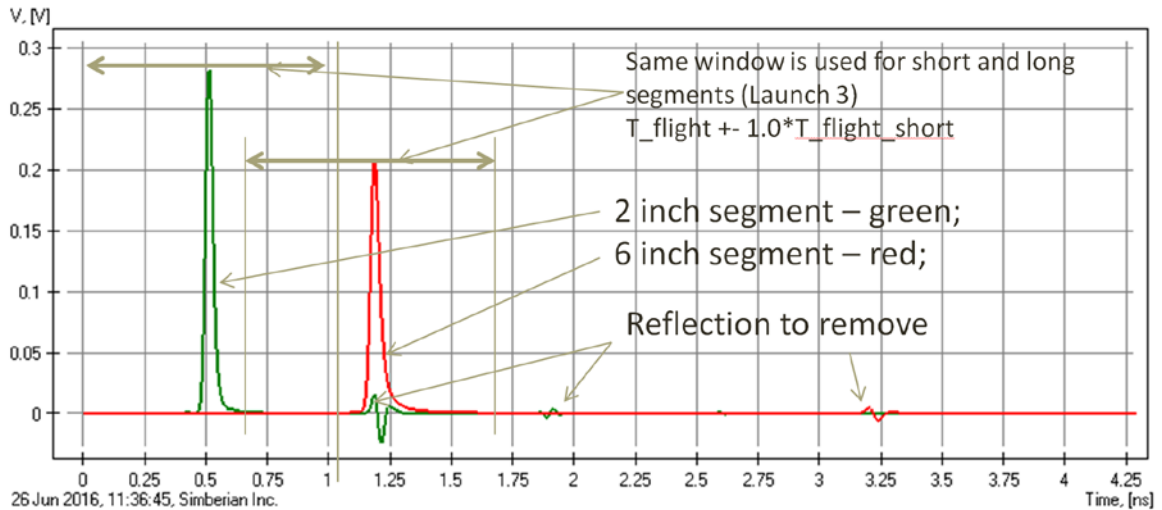


Fig. 7.6. Pulse responses of the 2 and 6 inch segments with launch 3 (bad). The oscillations caused by double reflection from the launches should be windowed as illustrated here.

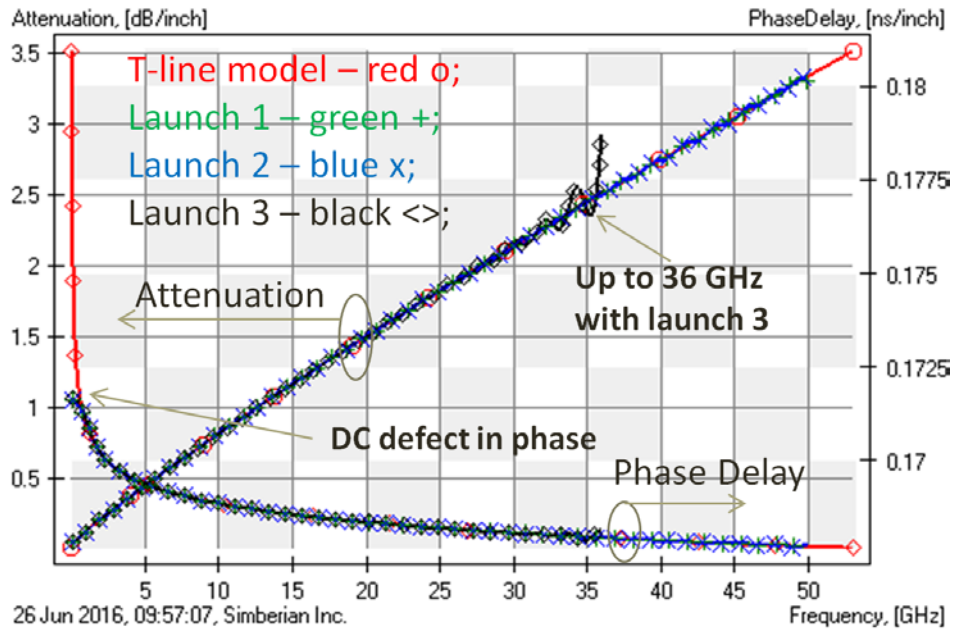


Fig. 7.7. Gamma as attenuation and phase delay extracted from TDTs of 2 and 6 inch segments equipped with different launches and with the windowing in time domain.

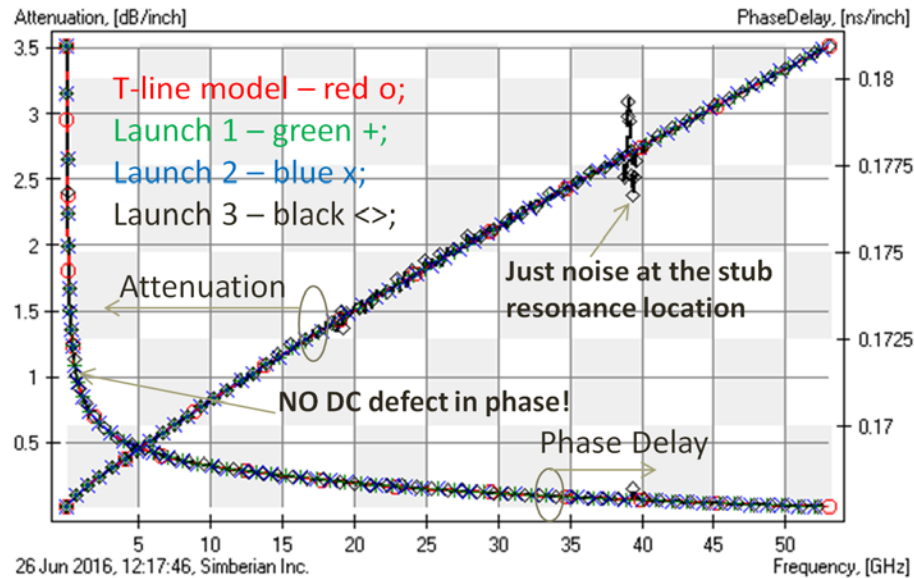


Fig. 7.8. Gamma as attenuation and phase delay extracted from S-parameters of 2 and 6 inch segments equipped with different launches.

Finally, let's use S-parameters of 2 and 6 inch segments with the three launches for Gamma extraction. The results are shown in Fig. 7.8. This is why we call this approach precise – the results practically overlap with the original t-line parameters. This is because the conversion of S-parameters into GMS-parameters is the complete de-embedding, unlike the windowing in the time domain. It gets rid of the reflection without any defects at lower and higher frequencies. It makes the precise procedure self-sufficient and suitable for the model identification with the separation of the dielectric and conductor losses. However, the T-resonator procedure can be used to double check the results and make adjustments to the cross-section if some discrepancies are observed.

We conclude that the extraction of Gamma from TDTs can tolerate substantial reflections from the launches – the perfect launch design is not necessary. Gamma extraction from S-parameters can handle practically any launch reflections. However, in both cases, some efforts are required to make the launch less sensitive to the manufacturing variations. A reflective launch may have very narrow gaps between planes and pads for instance. That can cause substantial dependency of the reflections from the manufacturing variations. That is translated into substantial non-identity of the launches that can affect the Gamma extraction. This has to be further investigated. Note that the low-frequency defects of Gamma extracted from TDT does not allow the dielectric and conductor roughness loss separation approach described for the precise technique earlier. Thus the T-resonator extraction complements it. Also, the final dielectric and conductor models in this technique are not point by point, but rather frequency-continuous with analytical continuations to DC and to infinity. It makes the whole approach much less sensitive to the observed oscillations and other defects. Most of the defects are simply fixed by the numerical model and the extracted material parameters are typically useful well above the last frequency point of the Gamma extraction.

8. Practical examples

To test the proposed Gamma-T technique, a number of test boards were designed and investigated. One of the test boards with launches designed for the Introbotix hand-held probes is shown in Fig. 8.1. The board stackup is similar to what is expected in the production environment. Optimization of launch and vias took about 2 hours of setup and analysis time in Simbeor electromagnetic signal integrity software [16].

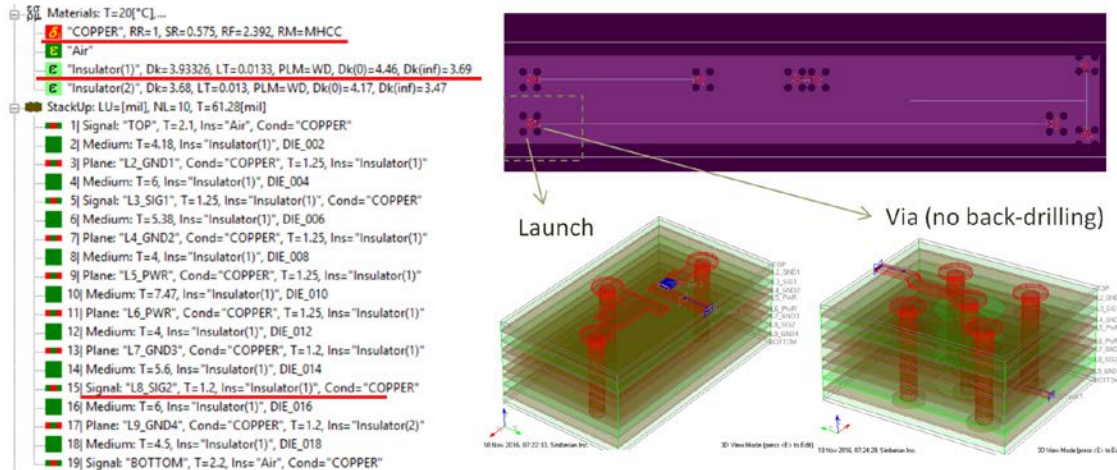


Fig. 8.1. Test board for Introbotix hand-held probes. Launch is optimized for the probe footprint for single-ended transmission line. Viahole transition from the microstrip to the strip line is optimized separately.

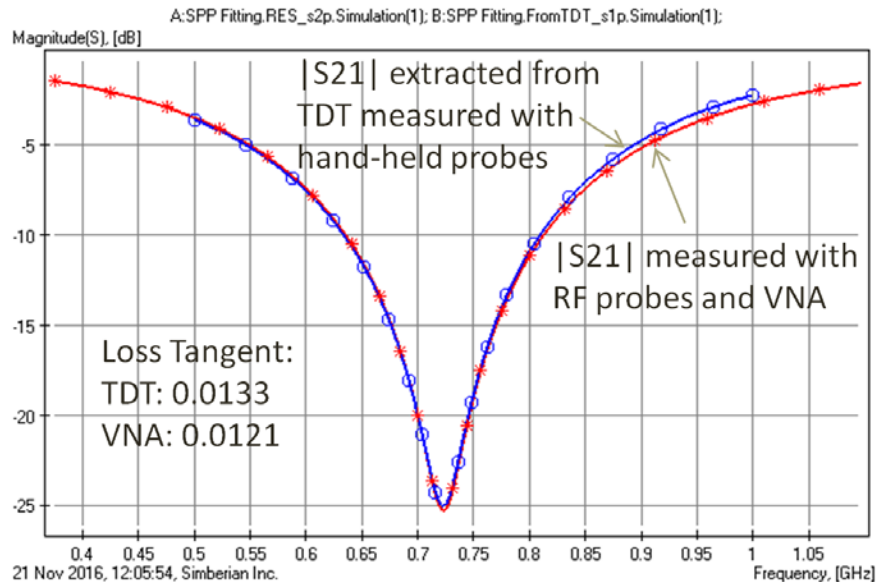


Fig. 8.2. Insertion loss of the T-resonator measured with RF probes and VNA (red curve with *) and with hand-held probes and TDR scope (blue curve with o).

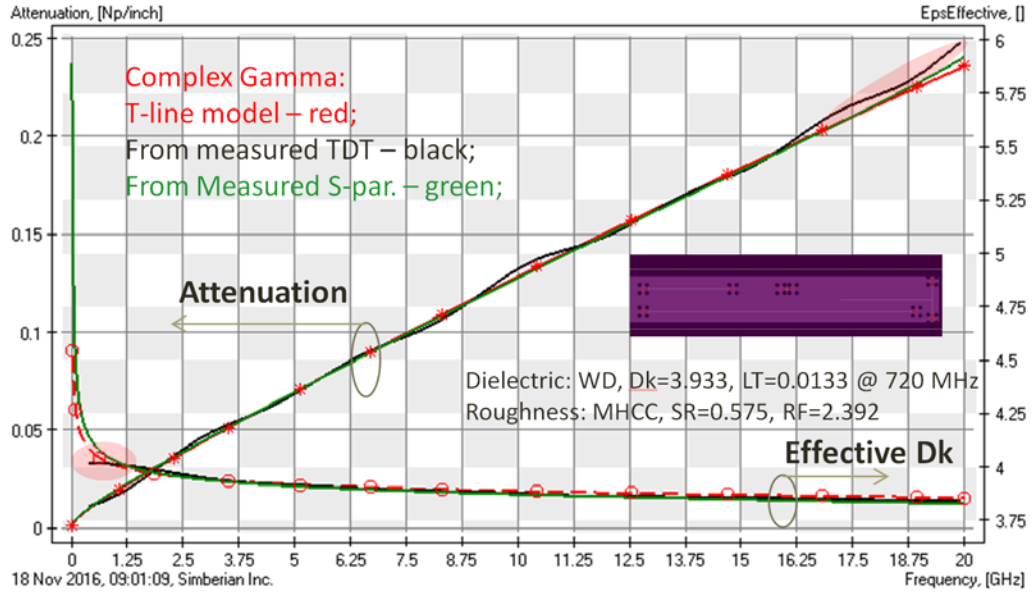


Fig. 8.3. Gamma as attenuation and phase delay extracted from TDTs measured with hand-held probes (black lines) and from S-parameters measured with VNA and probe station. Identified Wideband Debye model: $Dk=3.933$, $LT=0.0133$ @ 720 MHz. Identified conductor roughness Modified Hammerstad model: $SR=0.575$, $RF=2.392$.

The loss tangent was first identified with the T-resonator. The results are illustrated in Fig. 8.2. The resonance frequency is about 720 MHz. With the hand-held probes and TDR scope first the loss tangent is identified as 0.0133. To validate the results obtained with the TDT, we used RF probes and VNA and obtained $LT=0.0121$, that is within 10%. The insertion losses measured with VNA and TDR scope are very close as also shown in Fig. 8.2.

Next, Gamma was extracted from TDT measurements for two transmission lines and used to identify Wideband Debye dielectric model Dk at 720 MHz by matching computed and measured effective dielectric constant as illustrated in Fig. 8.3. Finally, conductor roughness model parameters are identified by matching the measured and computed transmission line attenuation as also illustrated in Fig. 8.3. The low and high frequency defects are simply smoothed out by the frequency continuous dielectric and conductor roughness models used in the field solver. Simbeor SFS quasi-static field solver was used for the dielectric and conductor roughness model identification. The models are re-usable in other quasi-static and electromagnetic solvers. To validate the results of the cost-effective technique, the same structures were investigated with the S-parameters measured with RF probes and VNA. Gamma extracted from the S-parameters with the precise technique is shown in Fig. 8.3 for comparison. The good correlation of the extracted Gamma with the transmission line with the identified material models is observed.

9. Conclusion

New Gamma-T technique for the material model validation or identification has been proposed here in two versions: the cost-efficient version with hand-held probes and TDR/TDT measurements for production floor and the precise version with S-parameters

measurement with VNA for validation in a lab. Sensitivity of both versions to the strip width variations and launch reflections is investigated. It is shown that the cost-effective technique is sufficiently robust and accurate up to 20 GHz. The precise version can be used for the material identification up to 50 GHz. The key to success in this project was using the right hardware (Introbotix probes) and software. Simbeor software was used to design test fixtures, extract Gamma from TDTs and S-parameter measurements and for the material model identification with the field solver models. The technique is ready for the industrial use or standardization.

10. References

1. [IPC-TM-650 Test Methods Manual #2.5.5.12.](#)
2. J. Hsu et al., Delta-L methodology for efficient PCB trace loss characterization, in Proc. Of 2014 9th IMPACT Conf., 22-24 Oct. 2014, p. 113 - 116.
3. Y. Shlepnev, Broadband material model identification with GMS-parameters, Proc. of 2015 IEEE 24st Conference on Electrical Performance of Electronic Packaging and Systems (EPEPS'2015), San Jose, 2015.
4. Y. Choi, C. Cheng, N. Godishala, Y. Damgaci, Estimating circuit board characteristics, application WO2016003445 A1, July 1st, 2014.
5. A. Deutsch, et al., Characterization of resistive transmission lines by short pulse propagation, - in IEEE Microwave and Guided Wave Letters, vol. 2, N 1, 1992.
6. Y. Shlepnev, Y. Choi, C. Cheng, Y. Damgaci, Drawbacks and Possible Improvements of Short Pulse Propagation Technique, Proc. of 2016 IEEE 25st Conference on Electrical Performance of Electronic Packaging and Systems (EPEPS'2016), pp. 141-143, October 23-26, 2016, San Diego, CA.
7. R.M. Djordjevic, V.D. Biljic, Likar-Smiljanic, T.K. Sarkar, Wideband frequency domain characterization of FR-4 and time-domain causality, IEEE Trans. on EMC, vol. 43, N4, 2001, p. 662-667.
8. Y. Shlepnev, C. Nwachukwu, Roughness characterization for interconnect analysis. - Proc. of the 2011 IEEE International Symposium on Electromagnetic Compatibility, Long Beach, CA, USA, August, 2011, p. 518-523.
9. P. G. Huray, O. Oluwafemi, J. Loyer, E. Bogatin, X. Ye, Impact of Copper Surface Texture on Loss: A Model that Works, DesignCon 2010.
10. M.Y. Koledintseva, A. Ramzadze, A. Gafarov, S. De, S. Hinaga, J.L. Drewniak, PCB conductor surface roughness as a layer with effective material parameters. – in Proc. IEEE Symp. on EMC, Pittsburgh, PA, USA, 2012, p. 138-142.
11. K.-P. Latti, et al, A Review of Microstrip T-resonator Method in Determination of Dielectric Properties Circuit Board Materials, Proceedings of the 2005 Instrumentation and Measurement Technology Conference, IMTC 2005, May 2005, Vol. 1, pp. 62- 66.
12. S. B. Cohn, Problems in Strip Transmission Lines, IRE Transactions MTT-2, March 1955, p. 119-126.
13. [Y. Shlepnev, A. Neves, T. Dagostino, S. McMorrow, Measurement-Assisted Electromagnetic Extraction of Interconnect Parameters on Low-Cost FR-4 boards for 6-20 Gb/sec Applications - the award-winning paper from DesignCon2009.](#)

14. M. D. Janezic, J. A. Jargon, Complex Permittivity Determination from Propagation Constant Measurements, IEEE Microwave and Guided Wave Letters, vol. 9, NO. 2, Feb. 1999, pp. 76-78.
15. [G. Brist, Design Optimization of Single-Ended and Differential Impedance PCB Transmission Lines](#), Intel Corp.
16. [Simbeor Electromagnetic Signal Integrity Software – Simberian Inc.](#)